Lasers in Manufacturing Conference 2019

Adaptive technique for signals in the monitoring of laser welding

Giuseppe D'Angelo[a*], Gianmarco Genchi[a], Giorgio Pasquettaz[a]

[a]*C.R.F. S.C.p.A., Strada Torino, 50, Orbassano 10043, Italy*

Abstract

Laser weld monitoring is usually based on the feedback from sensors (photodiodes, cameras) able to provide information about radiation from plume, the reflected laser light and the thermal condition of the melt. By using the optical emissions, it is possible to evaluate laser process quality, in particular, to find out the relationship between emission characteristics and weld quality characteristics. However, the optical signals detected during the laser welding are typically contaminated by different kind of noises that affect the sensor. To avoid this phenomenon, it is necessary to de-noise the signal for getting a "clean" signal. A plethora of inspection systems have being developed to improve weld quality and reduce overall costs. However, the signal analysis technique to be applied, for inferring information about the condition of the weld, is still an open field. This work presents a technique based on an adaptive method for cleaning up the signal, named Modified Singular Spectrum Analysis (MoSSA), combined with the Teager-Huang Transform (THT) for better inferring information about the condition of the weld. The proposed technique significantly improves components localization. For giving practical applicability to the proposed method, we compare the methods by analyzing signals detected during the laser welding, demonstrating the expected advantages.

Keywords: singular spectrum analysis; transient signal analysis; Teager Kaiser energy operator;

1. Introduction

Laser welding is increasingly used in industrial applications, because of the advantages it offers, such as high speed, high accuracy, low heat input and low distortion. As for any other fusion welding process, weld imperfections can occur. In the automotive industry, for instance, the demand for real-time monitoring

* Corresponding author. Tel.: +39 011 9083378
E-mail address: giuseppe.dangelo@crf.it

methods has become increasingly urgent since for reducing vehicle weight and improve fuel efficiency and safety, the development of lightweight and high-strength vehicles has prompted an increased use of advanced high strength steels (AHSS). These steels are galvanized in order to improve the surface corrosion resistance for automotive parts. It is still a great challenge the laser weld of galvanized steels in a zero-gap lap joint configuration. When laser welding of galvanized steels in a zero-gap lap-joint configuration, the zinc coating at the contact interface will vaporize; due to the lower boiling point (906 0C) of zinc as compared to the melting temperature of steel (above 1500 ^{0}C), the highly pressured zinc vapour expels the liquid metal out of the weld pool, resulting in blowholes and pores which dramatically decrease the mechanical properties of the weld [1-10].

Most common techniques in use today for process monitoring, employ sensors to record electromagnetic (EM) signals arising from the molten pool during welding, with the objective of correlating the output from the sensor to features such as weld penetration, the occurrence of pin holes, or weld shape. These systems have been developed to monitor laser welding in real-time and generally examine the laser-to-metal interactions to infer the quality of the weld itself.

By using different types of sensors, responding to different wavelengths of light, different aspects of the process or weld can be monitored, such as the weld pool temperature, the plasma above the weld pool and the level of back reflection, for instance. Through the optical emissions, it is possible to evaluate laser process quality, in particular, to find out the relationship between emission characteristics and weld quality characteristics.

Since these techniques are indirect, they require accurate signal interpretation and processing to infer information about the actual condition of the weld: the more accurate signal analysis technique, the better weld quality characterization [11-16].

Many signal analysis methods have been developed. These methods include, as example, power spectrum estimation and fast Fourier transform (FFT). However, these methods are based on the assumption of stationarity and linearity of the detected signals. Unfortunately, laser welding defects by their nature are time-localized transient events. To deal with non-stationary and nonlinear signals, time-frequency analysis techniques such as the Short-Time Fourier Transform (STFT) , Wavelet Transform (WT), Wigner-Ville distribution (WVD) are used [17-51]:

- the drawback with the STFT is the limitation between time and frequency resolutions
- the limitation of the wavelet analysis is its non-adaptive nature
- the difficulty with the WVD is the severe cross terms as indicated by the existence of negative power for some frequency ranges.

In this study, a new method has been developed for finding out the relationship between emission characteristics and weld quality characteristics. The developed method is based on Orthogonal Empirical Mode Decomposition (OEMD) and Teager–Kaiser Energy Operator (TKEO) algorithms [52-60]:

- the OEMD theory, developed by Huang and improved by CRF, decomposes the signal into a set of band-limited functions (orthogonal intrinsic mode functions, IMFs) and allows the extraction of instantaneous information from the signal.
- the Teager Kaiser energy operator estimates the instantaneous frequency and amplitude of the signal.

Figure 1 shows the algorithm blocks diagram using the OEMD and TKEO theories, on which, as example, the defects detection approach is based.

However, the optical signals detected during the laser welding are typically contaminated by different kind of noises that affect the photo-detector. To avoid this phenomenon, it is necessary to smooth and de-noise the signal for getting a “clean” signal. Although several methods have been developed to reduce the effect of noise, one of the most effective methods of dealing with noise contamination is to filter the noise out of the signal while retaining as much as possible of the region of interest in the frequency spectrum.

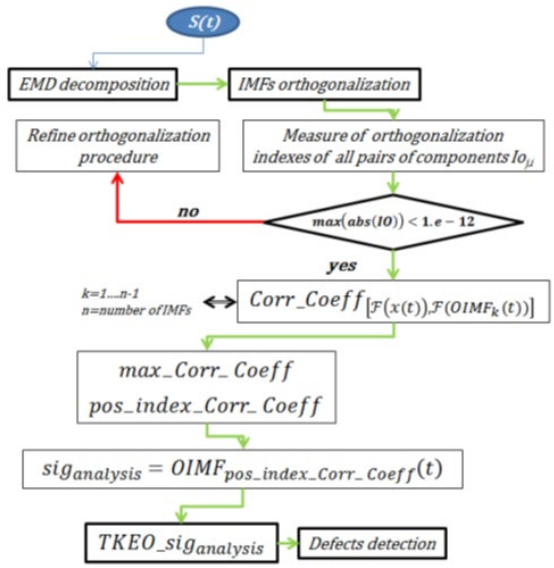

Fig.1. Algorithm blocks diagram using the OEMD and TKEO theories

The traditional method to de-noise process signals is to use digital Butterworth filters. Nonetheless, more advanced filtering techniques such as discrete wavelet transforms, Wiener filtering have also been used to that end. Although these methods have proven useful, their main drawback is the complexity of devising an automatic and systematic procedure, i.e., a mother wavelet function must be selected when using discrete wavelet transforms, the filtering function parameters must be chosen when using the Wiener filter, etc.

Singular spectrum analysis (SSA) is a novel non-parametric technique based on principles of multivariate statistics. The original time series is decomposed into a number of additive time series, each of which can be easily identified as being part of the signal, or as being part of the random noise. This way it's possible to get a clean signal without noise [61-65]. The SSA method is based on two parameters, window length and number of eigenvectors, which has to be set before starting the de-noising procedure. Certain choices of window lengths and number of eigenvectors (grouping strategy) lead to poor separation between trend and noise in the signal, i.e., trend components become mixed with noise components in the reconstruction of the signal.

The Modified Singular Spectrum Analysis (MoSSA) method, developed by CRF, overcomes the previous drawbacks and is intended to be a valid alternative to traditional digital filtering methods.

The purpose of this paper is to show how the application of OEMD and TKEO algorithms to properly denoised signals, allows to evaluate the quality of laser welded components without using any signal as reference.

The organization of this paper is as follow:

- Section I, reports the Modified Singular Spectrum Analysis (MoSSA)
- Section II, briefly presents the Orthogonal Empirical Mode Decomposition (OEMD) and the Teager–Kaiser Energy Operator (TKEO) methods
- Section III finally, illustrates the application of the OEMD & TKEO analysis to the signals detected during the welding of Ni 718 –BoP material, demonstrating its applicability to the proposed method.

2. Modified Singular Spectrum Analysis (MoSSA) method

2.1 *Singular Spectrum analysis (SSA)*

The main purpose of SSA is to decompose the original series into a sum of series, so that each component in this sum can be identified as either a trend, periodic or noise. This is followed by a reconstruction the original series. The SSA technique consists of two complementary stages: decomposition and reconstruction and both of which include two separate steps. At the first stage we decompose the series and at the second stage we reconstruct the original series and use the reconstructed series which is without noise. We provide a discussion on the methodology of the SSA technique. We consider the real-valued nonzero time series of sufficient length T Y_T=(y_1….y_T). Fix L ($L \leqslant T/2$), the window length, and let K=$T-L$+1.

Step 1 - *Computing the trajectory matrix (Embedding)*
This transfer a one-dimensional time series $Y_T=(y_1 \ldots . y_T)$ into the multi-dimensional series $X_1 \ldots \ldots X_K$ with vectors $X_i=(y_i \ldots . y_{i+L+1}) \in R^L$, where $K=T-L+1$.
The single parameter of the embedding is the *window length* L, an integer such that $2 \leq L \leq T$.
The result of this step is the trajectory matrix or Hankel matrix, (all the elements along the diagonal $i+j=const$ are equal)

$$\boldsymbol{X} = \left(x_{i,j}\right)_{i,j=1}^{L,K} = \begin{pmatrix} y_1 & y_2 & \ldots . & y_k \\ y_2 & y_3 & \ldots . & y_{k+1} \\ \ldots . & \ldots . & \ldots . & \ldots . \\ y_L & y_{L+1} & \ldots . & y_T \end{pmatrix} \qquad (2.1)$$

Step 2 - *Singular value decomposition of the trajectory matrix*
It can be proved that the trajectory matrix (or any matrix of that type) may be expressed as the sum of d rank-one elementary matrices $\boldsymbol{X} = E_1 + E_1 + \cdots E_d$, where d is the number of non-zero eigenvalues in decreasing order, λ_1,λ_2,…λ_d of the LxL matrix $\mathbf{S}$=$\boldsymbol{X} \cdot \boldsymbol{X^T}$.
The elementary matrices are given by:

$$\boldsymbol{E_i} = \sqrt{\lambda_i} \cdot \boldsymbol{U_i} \cdot \boldsymbol{V_i} \cdot \boldsymbol{T} \qquad (2.2)$$

for i=1,2,….,d, with $\boldsymbol{U_1}$,$\boldsymbol{U_2}$,…,$\boldsymbol{U_d}$ being the corresponding eigenvectors, and the vectors $\boldsymbol{V_i}$ being given by:

$$\boldsymbol{V}_i = \boldsymbol{X^T} \cdot \boldsymbol{U_i} \cdot (\lambda_i)^{-1} \qquad (2.3)$$

for i=1,2,….,d .The contribution of the first elementary matrices $\boldsymbol{E_i}$ to the norm of $\boldsymbol{X}$ is much greater than that of the last matrices. Therefore, it is likely that these last matrices represent noise in the signal. The plot of eigenvalues in decreasing order is called the singular spectrum, and gives the method its name.

Step 3 - *Grouping*
The next step consists in partitioning the set of indices {1,…,} into m disjoint subsets: I_1,…,I_m. Let $\boldsymbol{I}$=i_1,…, be one of these partitions. Then, the trajectory matrix $\boldsymbol{E}_I$corresponding to the set $\boldsymbol{I}$ is defined as E_I=E_{i1}+ +E_{i2}+⋯E_{ib}. Once the matrices have been calculated for the partitions established, I_1,…,I_m, the original time series trajectory matrix can be expressed as the sum of the trajectory matrices corresponding to each partition: $\boldsymbol{X}$=E_I=E_{I1}+ E_{I2}+⋯E_{Ib}.

Step 4 - *Reconstruction (diagonal averaging)*
In this step, each trajectory matrix $\boldsymbol{E_i}$ is transformed into a principal component of length $\boldsymbol{N}$ by applying a linear transformation known as diagonal averaging or Hankelization. To reconstruct each principal

component, the average along the diagonals $i+j=const$ is calculated. The diagonal averaging algorithm (Golyandina) is as follow: let Y be any of the elementary matrices $\boldsymbol{E_i}$ of dimension LxK, the elements of which are y, with $1 \le i \le L$, $1 \le j \le K$.
The time series $\boldsymbol{G}$ (principal component) corresponding to this elementary matrix is given by:

$$g_k = \begin{cases} \dfrac{1}{k+1}\displaystyle\sum_{m=1}^{k+1} y_{m,k-m+2} & for\ 0 \le k < L^*-1 \\ \dfrac{1}{L^*}\displaystyle\sum_{m=1}^{L^*} y_{m,k-m+2} & for\ L^*-1 \le k \le K^* \\ \dfrac{1}{N-K}\displaystyle\sum_{m=K-k^*+2}^{N-k^*+1} y_{m,k-m+2} & for\ K^* \le k < N \end{cases}$$

where $L^* = min(L,K)$, $K^* = max(L,k)$, and $N = L+K-1$.

It can be shown that the squared norm of each elementary matrix equals the corresponding eigenvalue, and that the squared norm of the trajectory matrix is the sum of the squared norms of the elementary matrices. The largest eigenvalues in the singular spectrum represent the high-amplitude components in the decomposition. Contrariwise, the low-amplitude noise components of the signal are represented in the singular spectrum by the smallest eigenvalues.

2.2 *Modified Singular Spectrum analysis (MoSSA)*

One of the drawbacks of SSA is the lack of a general criterion to select the values of the parameters L (window length) and the grouping strategy used in the algorithm.
Certain choices of window lengths and grouping strategy lead to poor separation between trend and noise in the signal, i.e., trend components become mixed with noise components in the reconstruction of the signal.
To overcome the uncertainty in what value L to select, we apply sequentially the Singular Value Decomposition step, starting from L=3:

- for each iteration, the RMS between the current and previous eigenvalue is calculated

$$RMS(1) = rms(\lambda_1 : \lambda_2)$$
$$RMS(2) = rms(\lambda_2 : \lambda_3)$$
$$\vdots$$
$$R(L-1) = rms(\lambda_{L-1} : \lambda_L)$$

- the minimum and its position is calculated based on defined halt criterion at iteration $[min, posmin] = m(RMS(1:L-1)) < \varepsilon = 1/100$

The convergence of this sequential procedure is such in that the percentage RMS difference between the current and previous signals in a given iteration is sufficiently small.

2.3 *Application to laser welding process signals*

The aim of this section is to demonstrate how the proposed method effectively smooths the signals detected during the laser welding. The data acquisition was performed with a NI CompactRIO multi-channel data acquisition board. High Strength Steel DP600 has been used for the trials. We firstly apply the Singular Spectrum Analysis, highlighting its own drawback, after that we demonstrate the effectiveness of the modified version.

Example #1 – Welding of High Strength Steel DP600 – overlapped samples, sampling frequency 32768 Hz

Figure 2 displays the signal (left) detected during the laser welding of overlapped HSS samples and the relative spectrum (right). Figure 3 displays up-left) de-noised signal, up-right) de-noised signal spectrum, bottom-left) residual noise, bottom-right) noise spectrum

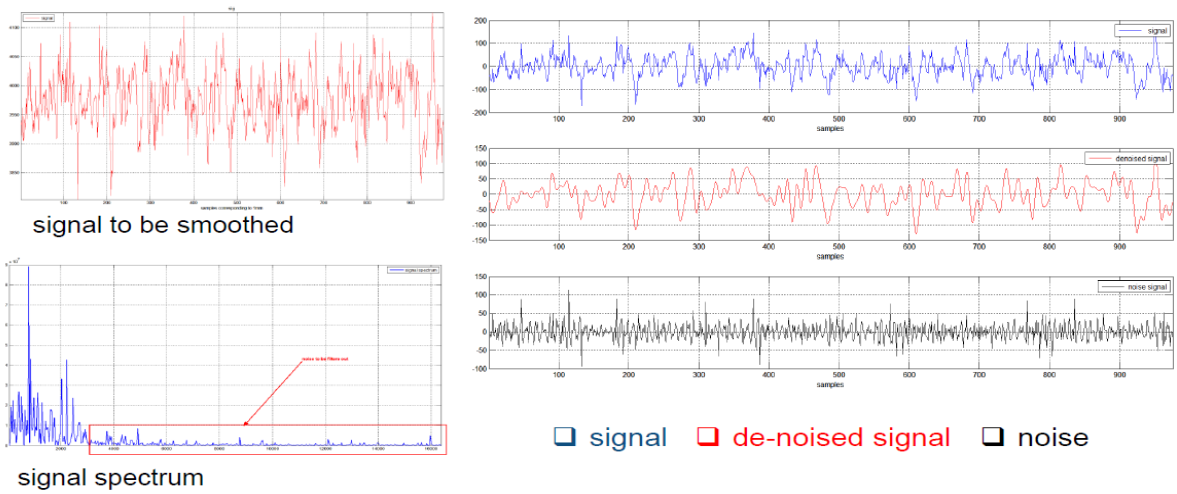

Fig.2. (up-left) raw signal, (bottom-left) spectrum, (right) denoised signal and noise

It should be noted, looking at the spectra shown in figure 3, the separation between the spectra. This condition ensures that the de-noised signal is not contaminated by noise. The Modified Singular Spectrum analysis method allows the smoothing of the signal without fixing any initial conditions.

3. Orthogonal Empirical Mode Decomposition (OEMD) method

The Empirical Mode Decomposition (EMD) has an assumption that any data consists of different simple intrinsic models of oscillations. Each intrinsic mode, no matter linear or not, represents an oscillation, which will have the same number of extrema and zero-crossings, and then the oscillation will be symmetric with respect to the local mean. Usually, the data may have many different oscillations which can be represented by the intrinsic mode functions (IMF) with following definition:

- in the whole dataset, the number of extrema and the number of zero-crossings must either equal or differ at most by one,
- at any point, the mean value of the envelope defined by the local maxima and the envelope defined by the local minima is zero.

An IMF is much more general than an oscillation mode because it has a variable amplitude and frequency as a function of time.

The components of the EMD are usually physically meaningful, for the characteristic scales are defined by the physical data.

3.1 *Orthogonal Empirical Mode Decomposition Method (OEMD)*

The EMD approach proposed by Huang can't ensure strict orthogonality in theory, and only indicate approximately orthogonality among each IMF in numerical value. Actually from some numerical examples we can find the degree of orthogonality is relatively imprecise. Leakage of energy will be happened if we estimate the local spectral density of non-stationary signals detected during the laser welding, and then the local spectral density cannot be regarded as the time-dependent spectral density of original signals.
To ensure the rigorousness of EMD, the IMFs from EMD should reconstruct the original signal. The IMFs can theoretically reconstruct the original signal. In order to check the orthogonality of IMFs from EMD, Huang et al. defined an overall index of orthogonality IO_T and a partial index of orthogonality for any two components IO_{jk} , as follows:

$$IO_T = \sum_{j=1}^{n+1}\sum_{\substack{k=1\\k\neq j}}^{n+1}\int_0^T c_j(t)\,c_k(t)dt \Big/ \int_0^T x^2(t)dt = \sum_{j=1}^{n+1}\sum_{\substack{k=1\\k\neq j}}^{n+1}\sum_{i=1}^{N} c_{ji}c_{ki} \Big/ \sum_{i=1}^{N} x_i^2 \qquad (3.1)$$

$$IO_k = \int_0^T c_j(t)c_k(t) \Big/ \int_0^T c_j^2(t)dt + \int_0^T c_k^2(t)dt = \sum_{j=1}^{N} c_{ji}c_{ki} \Big/ \sum_{i=1}^{N} c_{ji}^2 + c_{ki}^2 \qquad (3.2)$$

Furthermore, we defined an energy index to indicate the orthogonality of IMF components. The energy of original signal E_x and the energy of each IMF component are given by:

$$E_x = \int_0^T X^2(t)dt = \sum_{i=1}^{N} X_i^2 \qquad (3.3)$$

$$E_j = \int_0^T c_j^2(t)dt = \sum_{i=1}^{N} c_j^2 \ (j = 1, \dots, n+1) \qquad (3.4)$$

If the IMF components from EMD are exactly orthogonal to each other, the value of IO_T should be zeros, the total energy of decomposed signal E_{tot} should be invariable and the energy leakage between any two IMF components E_{jk} should be zero. Generally, because the IMFs from EMD aren't theoretically orthogonal, the value of orthogonality index is about from 10^{-2} to 10^{-3}. Therefore, Huang considered that there is almost orthogonal among IMFs.
However, numerical simulation demonstrated that owing to the minor error in orthogonality that Huang considered, there is actually severe energy leakage when applied EMD for the decomposition of time signals. In order to ensure the exact orthogonality of IMFs from EMD and no energy leakage due to EMD, a new method based on the Gram-Schmidt orthogonalization method referred as the orthogonal empirical mode decomposition (OEMD) has been proposed to improve the problem.
In order to demonstrate the orthogonality validity of IMF from EMD to OEMD, let's consider, as example, a temperature signal detected during the laser welding of polymers.

Table I shows the value of the orthogonality indexes for IMF and OIMF.

OIMF	c1	c2	c3	c4	c5	c6	c7
c1	0.50	-1.31E-18	1.63E-17	6.04E-18	-3.04E-18	1.37E-18	1.31E-18
c2	-1.31E-18	0.50	-2.12E-17	-8.54E-17	-3.09E-17	4.82E-18	-2.15E-17
c3	1.63E-17	-2.12E-17	0.50	-1.27E-17	7.60E-19	3.06E-17	-4.72E-18
c4	6.04E-18	-8.54E-17	-1.27E-17	0.50	-1.49E-17	-9.10E-19	4.09E-18
c5	-3.04E-18	-3.09E-17	7.60E-19	-1.49E-17	0.50	-3.32E-17	-1.03E-17
c6	1.37E-18	4.82E-18	3.06E-17	-9.10E-19	-3.32E-17	0.50	9.46E-17
c7	1.31E-18	-2.15E-17	-4.72E-18	4.09E-18	-1.03E-17	9.46E-17	0.50

IMF	c1	c2	c3	c4	c5	c6	c7
c1	5.00E-01	-2.26E-02	-8.87E-02	-1.02E-01	1.57E-02	3.56E-02	-1.11E-02
c2	-2.26E-02	5.00E-01	-5.55E-02	-2.27E-01	-6.22E-02	-1.29E-02	-8.23E-02
c3	-8.87E-02	-5.55E-02	5.00E-01	7.19E-02	-1.30E-02	2.78E-02	-1.08E-02
c4	-1.02E-01	-2.27E-01	7.19E-02	5.00E-01	-3.41E-02	-3.70E-03	-3.27E-02
c5	1.57E-02	-6.22E-02	-1.30E-02	-3.41E-02	5.00E-01	-9.30E-03	5.31E-02
c6	3.56E-02	-1.29E-02	2.78E-02	-3.70E-03	-9.30E-03	5.00E-01	-1.00E-01
c7	-1.11E-02	-8.23E-02	-1.08E-02	-3.27E-02	5.31E-02	-1.00E-01	5.00E-01

Comparing the indexes between IMF and OIMF, we can see that the orthogonalization process has provided the expected results. The IMFs indexes match with the Huang theory (the value of orthogonality index is about from 10^{-2} to 10^{-3}, whereas the OIMFs indexes are closed to zero, as expected.

Table II shows the energy leakage between any pair of IMF components: without orthogonalising the IMFs, severe leakage is present.

E_IMF(ci*cj)	c1	c2	c3	c4	c5	c6	c7
c1	7.19E+02	-1.45E+02	-1.11E+02	-3.39E+02	2.34E+01	4.59E+01	-1.12E+02
c2	-1.45E+02	5.72E+03	-3.47E+02	-1.89E+03	-4.04E+02	-8.09E+01	-1.24E+03
c3	-1.11E+02	-3.47E+02	5.28E+02	2.26E+02	-1.69E+01	3.05E+01	-1.06E+02
c4	-3.39E+02	-1.89E+03	2.26E+02	2.61E+03	-1.15E+02	-1.19E+01	-3.92E+02
c5	2.34E+01	-4.04E+02	-1.69E+01	-1.15E+02	7.72E+02	-1.24E+01	5.38E+02
c6	4.59E+01	-8.09E+01	3.05E+01	-1.19E+01	-1.24E+01	5.70E+02	-9.95E+02
c7	-1.12E+02	-1.24E+03	-1.06E+02	-3.92E+02	5.38E+02	-9.95E+02	9.36E+03

E_OIMF(ci*cj)	c1	c2	c3	c4	c5	c6	c7
c1	9.20E+00	0.00E+00	0.00E+00	0.00E+00	0.00E+00	0.00E+00	0.00E+00
c2	0.00E+00	4.68E+02	0.00E+00	0.00E+00	0.00E+00	0.00E+00	0.00E+00
c3	0.00E+00	0.00E+00	2.13E+02	0.00E+00	0.00E+00	0.00E+00	0.00E+00
c4	0.00E+00	0.00E+00	0.00E+00	2.41E+02	0.00E+00	0.00E+00	0.00E+00
c5	0.00E+00	0.00E+00	0.00E+00	0.00E+00	1.44E+03	0.00E+00	0.00E+00
c6	0.00E+00	0.00E+00	0.00E+00	0.00E+00	0.00E+00	3.24E+02	0.00E+00
c7	0.00E+00	0.00E+00	0.00E+00	0.00E+00	0.00E+00	0.00E+00	6.67E+03

3.2 Teager–Kaiser Energy Operator (TKEO) method

Signals may represent a broad variety of phenomena. In many applications, signals are directly related to physical quantities capturing energy and power in a physical system. The concept of signal energy is of primary importance in the design of continuous and discrete domain systems. This work is interested in signals provided by sensors and thus, to the energy associated with these signals. In the real world, we always transmit signals with finite total energy $0 < Ex < +\infty$ (or with finite average power) representing the amount of energy contained in signal *x(t)*. The quantity *Ex* should be independent of the method used to calculate it. Engineers refer to such signals as having finite total energy, although *Ex* is not necessarily the *physical* energy of the signal *x(t)*. For example, the total energy of the source system modeled as a mass suspended by a spring of a constant stiffness required to produce a simple undamped harmonic oscillation is calculated by the sum of the kinetic energy of the mass and the potential energy in the spring. By studying the second order differential associated to this harmonic oscillator, it is easy to show that a simple sinusoidal varies as a function of both amplitude and oscillation frequency of the signal *x(t)*, which is quite different from simple squaring of the signal magnitude, $x^2(t)$. It is this source modeling that is used for characterizing *x(t)* by amplitude and frequency.

In their work on non-linear speech modeling, Herbert and Shushan Teager pointed out the dominance of modulation as a process in the speech production [8,9]. Based on the Teager's work, Kaiser proposed an energy measure that includes both the amplitude and the frequency of the signal [3]. This measure is often referred to as the Teager–Kaiser (TK) energy operator. Using the conventional view of the energy, it is easy to see that two tones at 10 Hz and 1000 Hz of unit-amplitude have the same energy.

However, the energy required to produce the signal of 1000 Hz is much greater than that for the 10 Hz signal. Using TK definition of energy, the two tones show different energy. This definition highlights the concept of signal energy from the point of view of the generation of the signal and emphasizes the importance of analyzing signals from the energy aspect of the system needed to produce them.

The Teager-Kaiser Energy Operator (TKEO), $\Psi[.]$, in the discrete case, is defined as:

$$\Psi_d[x(n)] = x_n^2 - x_{n+1}\,x_{n-1} \qquad (3.6)$$

4. Application of OEMD & TKEO to de-noised signals

Material and Laser equipment

Material	Thickness (mm)	Joint Configuration	Optical Sensor	Pre-welding preparation
Nickel (Ni) alloy 718	2.1 and 3.6	Butt and Bead-on-Plate (BoP)	IDM and Photodiode	• Abraded and acetone degreased • Dry machined square edges
DC01 mild steel	1.2	Lap	IDM	Acetone degreased
S355 Medium strength structural steel	6	Butt	Photodiode	Disc grinded and acetone degreased

Laser system

Laser	Multi-kW fibre laser
Wavelength	1070µm
Operation Mode	Continuous-wave
BPP, mm.mrad	~6
Fibre Diameter [µm]	150, 200
Collimating lens [mm]	160, 100
Focussing lens [mm]	160, 250
Spot size [µm]	200 or 300

Ranges of the parameters used in laser trials

Material	Speed (m/min)	Power (kW)	Focus (mm)
Ni 718	1.5-3	1 - 4	+6 to -16
DC01	3 - 4	1 – 5	-2
S355	1.5-3.0	5.0-7.5	+4 to -16

Monitoring equipment - Photodiodes

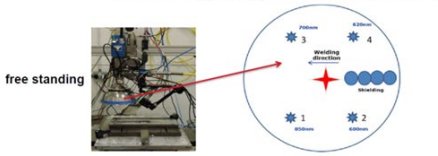

Ni 718 – Butt weld

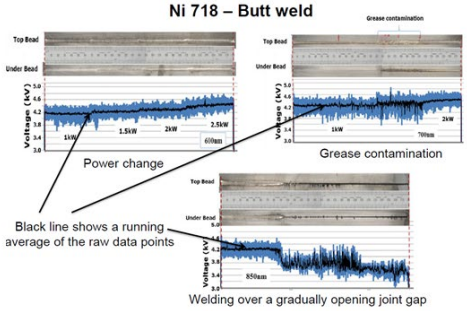

Ni 718 – BoP; Internal porosity

the arrows indicate **some locations where peaks in the signal data appeared to be in the proximity of the pores**

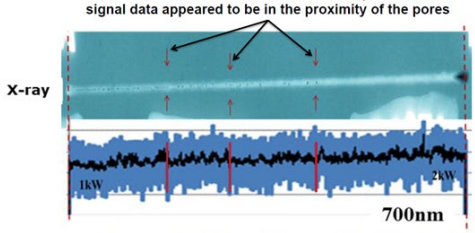

laser power ramped up from 1 to 2kW as welding proceeded, **to increase the level of penetration and correspondingly decrease the internal porosity content**

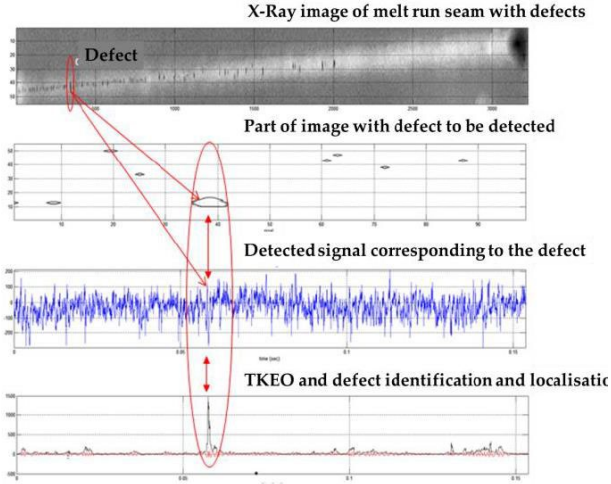

OIMF to correlate photodiode signal data to pores occurring within a melt run in nickel 718 alloy

- The OEMD decompose the signal into a set of band-limited functions and allows the extraction of instantaneous information from signal
- The TKEO estimates the instantaneous frequency and amplitude of the signal

5. Conclusions

This paper introduces a Modified Singular Spectrum Analysis (MSSA) for de-noising signals detected, as example, during the laser welding process. The proposed method is derived from the well-established Singular Spectrum Analysis, a novel non-parametric technique for smoothing and de-noising the detected signals. The MSSA method aims to overcome the uncertainty in what window length value to select and what number of eigenvectors to choose. The examples have demonstrated the effectiveness of the proposed

method. Besides the paper shows how the application of OEMD and TKEO algorithms to properly denoised signals, allows to evaluate the quality of laser welded components without using any signal as reference.

References

1. Akhter R., Steen W. M. and Cruciani D. (1988): 'Laser welding of zinc-coated steel'. Proceedings of the 5th International Conference on Lasers in Manufacturing, Stuttgart, West Germany, September 13-14.Clark, T., Woodley, R., De Halas, D., 1962. Gas-Graphite Systems, in *"Nuclear Graphite"* R. Nightingale, Editor. Academic Press, New York, p. 387.
2. Su-Jin Lee, Seiji Katayama, Yousuke Kawahito, Keisuke Kinoshita, Jong-Do Kim (2013): 'Weldability and keyhole behavior of Zn-coated steel in remote welding using disk laser with scanner head '. Journal of laser applications, volume 25, number 3
3. B.J. Aalderink, R.G.K.M. Aarts, J.B. Jonker, J. Meijer (2005): 'Weld Plume Emissions During Nd:YAG Laser Welding'. Proceedings of the Third International WLT-Conference on Lasers in Manufacturing 2005,Munich, June 2005
4. H. Springer, A. Szczepaniak, D. Raabe (2015); 'On the role of zinc on the formation and growth of intermetallic phases during interdiffusion between steel and aluminium alloys'. Article in Acta Materialia · September 2015
5. S. Katayama, "Laser welding," Bull. Iron Steel Inst. Jpn. 17(1), 18–29 (2012) (in Japanese).
6. L. Mei, G. Chen, X. Jin, Y. Zhang, and Q. Wu, 2009) ,'Research on laser welding of high-strength galvanized automobile steel sheets', Opt. Laser Eng. 47(11), 1117–1124 (2009).
7. R. Akhter, K. G. Watkins, and W. M. Steen, 'Electrochemical characterisation of the laser welded zinc coated steel', Mater. Lett. 9(12), 550–556 (1990).
8. KITANI Yasushi, OI Kenji, TAMAI Yoshikiyo (2015), 'Application of Laser Welding Technologies to Automotive Bodies' . JFE TECHNICAL REPORT, No. 20 (Mar. 2015)
9. Xiangzhong Jin, Yuanyong Cheng, Licheng Zeng, Yufeng Zou, and Honggui Zhang (2012), 'Multiple Reflections and Fresnel Absorption of Gaussian Laser Beamin an Actual 3D Keyhole during Deep-Penetration LaserWelding'.Hindawi Publishing Corporation International Journal of Optics Volume 2012, Article ID 361818, 8 page 8
10. S. Huber, J. Glasschroedera, M. F. Zaeh (2011), 'Analysis of the Metal Vapour during Laser Beam Welding'. Physics Procedia 12 (2011) 712–719
11. Michael F. Zaeh, Sonja Huber (2011), 'Characteristic line emissions of the metal vapour during laser beam welding'. Prod. Eng. Res. Devel. (2011) 5:667–678
12. R. Olsson, I. Eriksson, J. Powell and A.F.H. Kaplan (2009), 'Pulsed laser weld quality monitoring by the statistical analysis of reflected light'. LIM2009
13. B. N. Bad'yanov, A. A. Elizarov and Yu. F. Kolupaev (2003), 'APPLICATION OF THE STEP-BY-STEP APPROXIMATION METHOD FOR THE COMPUTER CONTROL OF LASER WELDING PROCESSES'. Measurement Techniques, Vol. 46, No. 2, 2003
14. P. Norman, I. Eriksson, A. F. H. Kaplan, 'MONITORING LASER BEAM WELDING OF ZINC COATED SHEET METAL TO ANALYZE THE DEFECTS OCCURRING'. Luleå University of Technology, Luleå, Sweden
15. Fanrong Kong, Junjie Ma, Blair Carlson, Radovan Kovacevic, 'Real-time monitoring of laser welding of galvanized high strength steel in lap joint configuration '.Optics & Laser Technology 44 (2012) 2186–2196
16. I. Eriksson, J. Powell, A.F.H. Kaplan,(2010),' Signal overlap in the monitoring of laser welding'. MEASUREMENT SCIENCE AND TECHNOLOGY Meas. Sci. Technol. 21 (2010) 105705
17. Giuseppe D'Angelo, Giorgio Pasquettaz, Andrea Terreno (2006),' IMPROVING THE ANALYSIS OF LASER WELDING PROCESS BY THE REASSIGNED TIME-FREQUENCY REPRESENTATIONS'. ICALEO 2006
18. J. B. Allen and L. R. Rabiner (1977), 'A unified approach to short-time Fourier analysis and synthesis', in Proc. IEEE, vol. 65, pp. 1558-1566.
19. L. Cohen (1966), 'Generalized phase space distribution functions', J. Math Phys, vol. 7, no. 5, pp. 781-786.
20. B. Escudié and J. Gréa (1976), 'Sur une formulation générale de la représentation en temps et en fréquence dans I' analyse des signaux d'énergie finie'. K. Acad. Sci. vol. 283, pp. 1049-1051. (in French).
21. J. Ville (1948), 'Théorie et applications de la notion de signal analytique'. Câbles et Transmissions. vol. 2A. pp. 66-74. (in French)
22. T. A. C. M. Claasen and W. F. G. Mecklenbrauker, 1980 'The Wigner distribution, a tool for time-frequency analysis, Part I: Continuoustime signals." vol. 35. no. 3. pp. 217-250: "Part 11: Discrete-time signals," vol. 35, no. 4/5, pp. 276300; "Part 111: Relations with other time- frequency signal transformations," Philips J. Res., vol. 35, no. 6, pp. 372-389.
23. L. Cohen (1989) 'Time-frequency distributions. A review,' in Proc. IEEE, vol. 77, pp. 941-981.
24. F. Hlawatsch and G. F. Boudreaux-Bartels (1992). "Linear and quadratic time-frequency signal representations," IEEE Signal Processing Mag., pp. 21-67

25. H. I. Choi and W. J. Williams (1989) “Improved time-frequency representation of multicomponent signals using exponential kernels,” IEEE Trans. Acoust., Speech, Signal Processing, vol. 37, pp. 862-871.
26. P. Flandrin and W. Martin (1984). “A general class of estimators for the Wigner-Ville spectrum of nonstationary processes” in Systems Analysis and Optimization of Systems, Lecture Notes in Control and Information Sciences. Berlin, Vienna, New York Springer-Verlag, pp. 15-23.
27. A. Papandreou and G. F. Boudreaux-Bartels (1992) ,“Distributions for time-frequency analysis: A generalization of Choi-illiams and the Buttervorth distributions,” in Proc. IEEE ICASSP, vol. 5, pp.181-184.
28. J. Jeong and W. J. Williams (1992) “Kernel design for reduced interference distributions,” IEEE Trans. Signal Processing, vol. 40, pp. 402-412.
29. S. Qian and J. M. Moms (1992) “Wigner distribution decomposition and cross-terms deleted representation,” Sig. Processing, vol. 27, no. 2, pp. 125-144.
30. S. Mallat and 2. Zhang (1992) “Adaptive timefrequency decomposition with matching pursuits,” in Proc. IEEE Sig. Processing Int. Symp. Time-Frequency and Time-Scale Anal., pp. 7-10.
31. M. Sun, C. C. Li, L. N. Sekhar, and R. J.Sclabassi (1989) “Elimination of the crosscomponents of the discrete pseudo Wigner-Ville distribution via image processing,” in Proc. IEEE ICASSP, pp. 2230-2233.
32. H. Oung and J. M. Reid (1990) “The Analysis of non-stationary Doppler spectrum using a modified Wigner-Ville distribution,” Int. Con$ IEEE EMBS, vol. 12, no. 1, pp. 460-461.
33. F. Auger and C. Doncarli (1989) “Un algorithme d’élimination des termes d’interférence de la transformée de Wigner-Ville,” Colloque Gretsi 89, pp. 99-102, (in French).
34. F. Auger (1991) “Représentations tempsfréquence des signaux non-stationnaires: Synthèse et contributions,” thèse de doctorat, Ecole Centrale de Nantes, (in French).
35. K. Kodera, C. de Villedary, and R. Gendrin (1976) “A new method for the numerical analysis of time-varying signals with small BT values,” Phys.Earth Planet. Interiors, no. 12, pp. 142-150.
36. K. Kodera, R. Gendrin, and C. de Villedary (1986) “Analysis of time-varying signals with small BT values,” IEEE Trans. Acoust., Speech, SignalProcessing, vol. ASSP-34, pp. 6476.
37. F. Auger, P. Flandrin (1995) “Improving the Readability of Time-Frequency and Time-Scale Representations by the Reassignment Method” IEEE Transaction On Signal Processing , vol.43, no. 5 May.
38. L. Li, D.J. Brookfield and W.M. Steen, Plasma charge sensor for in-process, non-contact monitoring of the laser welding process, Meas. Sci. Tech. Vol. 7(4) (Steen), pp. 615-26.
39. H. Luo, H. Zeng, L. Hu, X. Hu and Z. Zhou, Application of artificial neural network in laser welding defect diagnosis, Journal of Material Processing Technology, Vol. 170 (2005), pp. 403-11.
40. B. Venkatraman, B. Raj and M. Menaka, Online infrared detection of inclusions and lack of penetration during welding, Materials Evaluation, Vol. 63 (9) (2005), pp. 933-37.
41. A. Ancona, V. Spagnolo, P.M. Lugara and M.Ferrara, Optical sensor for real-time monitoring of CO2 laser welding process, Applied Optics, Vol. 40 (33) (2001), pp. 6019-25
42. B. Sung-Hoon, K. Min-Suk, P. Seong-Kyu, C. Chin-Man, K. Cheol-Jung and K. Kwang-Jung, Autofocus Control and Weld Process Monitoring of Laser Welding using Chromatic Filtering of Thermal Radiation, Meas. Sci. Tech., Vol. 11 (2000), pp.1772-77
43. P. G. Sanders, J. S. Keske, G. Kornecki, and K. H. Leong. Real-time Monitoring of Laser Beam Welding Using Infrared Weld Emissions. TechnologyDevelopment Division Argonne National LaboratoryArgonne, IL 60439 USA.
44. Chen, H. B., Li, L., Brookfield, D. J., Williams, K., and Steen, W. M. (1991). Laser process monitoring with dual wavelength sensors. In: Proc. ICALEO 91, San Jose, CA. Orlando, FL: Laser Institute of America, SPIE 1722, pp. 113-122.
45. Bagger, C., Miyamoto, I., Olsen, F., and Maruo, H. (1991). On-line control of the CO2 laser welding process. In: Beam Technology Conference Proceedings, Karlsruhe, Germany, March 13-14, DVS-Berichte 135, pp. 1-6.
46. Olsen, F.O., Jørgensen, H., Bagger, C., Kristensen, T., and Gregersen, O. (1992). Recent investigations in sensorics for adaptive control of laser cutting and welding. In: Proc. LAMP2, Nagoka, Japan: High Temperature Society of Japan, pp. 405-414.
47. Chang, D. U. (1994). Monitoring laser weld quality in real time. Indust. Laser Rev. 15-16,November.
48. Maischner, D., Drenker, A., Seidel, B., Abels, P., and Beyer, E. (1991). Process control during laser beam welding. In: Proc. ICALEO 91, San Jose, CA. Orlando, FL: Laser Institute of America, SPIE 1722, pp. 150-155.
49. G. D’Angelo, G. Pasquettaz, A. Terreno (2007). Laser process monitoring at FIAT group. In: Proc. EALA 07 - Bad Nauheim/Frankfurt, Germany, 30/31 January 2007.
50. C.Alippi, G.D’Angelo, V.Piuri et al (2003). Composite techniques for quality analysis in automotive laser welding. CIMSA 2003 – Lugano, Switzerland, 29-31 July 2003.
51. G. D’Angelo, G. Pasquettaz, A. Terreno (2006). Improving the analysis of laser welding process by the reassigned time-frequency representations. In: Proc. ICALEO 06, Scottsdale, AZ.

52. Ali Akbar Tabrizi, Luigi Garibaldi, Alessandro Fasana, Stefano Marchesielo (2014), 'Ensemble Empirical Mode Decomposition (EEMD) and Teager-Kaiser Energy Operator (TKEO) Based Damage Identication of Roller Bearings Using One-Class Support Vector Machine'. HAL Id: hal-01022990 , https://hal.inria.fr/hal-01022990
53. Pawel Stepien (2014), 'Sliding Window Empirical Mode Decomposition -its performance and quality'. Stepien EPJ Nonlinear Biomedical Physics 2014, 2:14, http://www.epjnonlinearbiomedphys.com/content/2/1/14
54. Zhaohua Wu and Norden E. Huang (20039, 'A Study of the Characteristics of White Noise Using the Empirical Mode Decomposition Method'. 2NASA Goddard Space Flight Center Code 971 Greenbelt, MD 20771
55. Eivind Kvedalen (2003), 'Signal processing using the Teager Energy Operator and other nonlinear operators', University of Oslo Department of Informatics
56. Olav B. Fosso, Marta Molinas, (2017), 'Method for Mode Mixing Separation in Empirical Mode Decomposition'. IEEE, arXiv:1709.05547v1 [stat.ME] 16 Sep 2017
57. Norden E. Huang, Zheng Shen, Steven R. Long, Man l i C. W u, Hs ing H. Shih, Quanan Zheng, Nai-Chyuan Yen, Chi Chao Tung and Henry H. Liu (1996), 'The empirical mode decomposition and the Hilbert spectrum for nonlinear and non-stationary time series analysis'. Proc. R. Soc. Lond. A (1998) 454, 903–995
58. Denis Donnelly (2008), 'Enhanced Empirical Mode Decomposition'. Computational Science and Its Applications – ICCSA 2008 pp 696-706
59. Donghoh Kim and Hee‑Seok Oh(2016), 'Empirical mode decomposition with missing values'. Kim and Oh SpringerPlus (2016) 5:2016, DOI 10.1186/s40064-016-3692-1
60. Sonam Maheshwari and Ankur Kumar (2014),' Empirical Mode Decomposition: Theory & Applications'. International Journal of Electronic and Electrical Engineering. ISSN 0974-2174 Volume 7, Number 8 (2014), pp. 873-878
61. N. Golyandina, V. Nekrutkin, and A. Zhigljavsky (2001), 'Analysis of Time Series Structure: SSA and Related Techniques'. CHAPMAN& H ALL/CRC. BocaRaton London New York Washington, D.C.
62. Juan Bogalo and Pilar Poncela and Eva Senra (2017), ' Automatic Signal Extraction for Stationary and Non-Stationary Time Series by Circulant SSA. Online at https://mpra.ub.uni-muenchen.de/76023/ MPRA Paper No. 76023, posted 8 January 2017 09:01 UTC
63. J. B´ogalo, P.Poncela and E. Senra (2018), 'Strong Separability in Circulant SSA'. https://www.researchgate.net/publication/325343422
64. Hassani, Hossein (2007): 'Singular Spectrum Analysis: Methodology and Comparison'. Published in: Journal of Data Science , Vol. 5, No. 2 (1 April 2007): pp. 239-257.
65. Hossein Hassan, SaeedHeravi, AnatolyZhigljavsky (2009), 'Forecasting European industrial production with singular spectrum analysis. International Journal of Forecasting Volume 25, Issue 1, January–March 2009, Pages 103-118